PHYSICAL REVIEW B VOLUME 60, NUMBER 23 15 DECEMBER 1999-I

Theoretical investigation of hydrogen- and halogen-terminated *c*-BN (111) clusters

B. Mårlid, K. Larsson, and J.-O. Carlsson
Department of Inorganic Chemistry, Ångström Laboratory, Uppsala University, Box 538, S-751 21 Uppsala, Sweden

(Received 30 March 1998; revised manuscript received 28 July 1999)

The surface stabilizing properties of different species X ($X=\mathrm{H,F,Cl,Br}$) on B(111) and N(111) *c*-BN cluster surfaces, have been investigated theoretically within the density-functional theory method. Calculated adsorption energies indicated that all species were found efficient in terminating the different cluster surfaces. However, Br species induce large sterical hindrances and thus disable the stabilization of especially a N(111) surface. For comparison, the surface stabilization properties of H and F on crystalline surfaces were also investigated. These species were, with one exception, even more efficient as surface stabilizing agents. However, there was hardly any effect for the adsorption of F on the crystalline N(111) compared to the corresponding smaller cluster surface. The adsorbed H and F species on the crystalline B(111) and N(111) surfaces, respectively, have been found, with one exception, to have a large possibility for surface migration and/or gas-phase abstraction. The F species adsorbed to the B(111) surface will most probably block the growth sites on that very surface. [S0163-1829(99)14547-8]

I. INTRODUCTION

Due to important industrial and technical applications, thin films of boron nitride (BN) have in recent years been investigated both theoretically and experimentally.[1,2] Cubic boron nitride (*c*-BN) exhibits many interesting properties similar to diamond, e.g., extreme hardness (second only to diamond), large band gap, low dielectric constant, and high thermal conductivity.[2] BN is isoelectronic to diamond and exists in four different phases.[3] There are two sp^2-hybridized phases (hexagonal; being isostructural to graphite, and rhombohedral) and two sp^3-hybridized phases (cubic with a zincblende structure and wurtzitic with a lonsdaleite structure).[4] Only the hexagonal form occurs in nature.

Cubic BN is generally grown in bulk crystal form from hexagonal BN under high pressure and high temperature (HPHT).[1,3,5] Deposition techniques for growth of BN thin films include both chemical vapor deposition (CVD) and physical vapor deposition (PVD) methods. Using thermally activated or hot-filament assisted CVD, the films presently become a multiphase mixture of amorphous (*a*-BN), turbostratic poorly crystallized sp^2-hybridized BN (*t*-BN) and *h*-BN.[1,3,6] In plasma-enhanced CVD (PECVD), BN films have been deposited with a high degree of the cubic phase.[7,8] Common for the different PECVD methods is the high concentration of electrons and radicals connected with the plasma, whether it be hydrogen-, halogen-, or any B- or N-containing radical species. Also the hot-filament method is known for producing a radical-rich environment.[9] Other successful methods for obtaining films with a high percentage of *c*-BN have involved simultaneous, high flux irradiation of ions on the growing film [either ion-beam-assisted deposition (IBAD), ion plating, rf sputtering, or PECVD with a biased substrate].[10–14] The ion-assisted PECVD or PVD films all show the same growth pattern. First, there's a few nanometer thick layer of amorphous BN, followed by a highly oriented layer (2–5 nm) of turbostratic BN. Then follows a nanocrystalline, almost single-phase, growth of *c*-BN.[4,15–18] The intrinsic, biaxial compressive stress induced during formation of *c*-BN may lead to poor adhesion and cracking of the films.[14,19] However, a high stress level is thought to be necessary to form the cubic phase.[18,20]

Several theoretical reports have been made as comparative studies between *c*-BN and diamond deposition.[21–23] For thermodynamic reasons, they role out the addition of hydrogen as a surface stabilizer and etchant in *c*-BN deposition. This is also confirmed experimentally in different PVD methods such as substrate-biased plasma methods involving sputtering of well-crystallized BN.[22–24] However, several contradictory investigations have reported hydrogen in a plasma, both as an etchant of sp^2-hybridized BN and as a stabilizer of the cubic phase.[25–28] Furthermore, it is reported that sp^2-hybridized BN is etched preferentially in comparison to sp^3-hybridized material by a BF_3/Ar gas mixture in a microwave plasma, and by a $BCl_3/N_2/H_2/Ar$ gas mixture in a rf plasma as well as in a hot-filament H_2/CH_4 gas environment,[29–31] whereas the stabilizing effects of hydrogen and halogens in diamond CVD have been investigated both theoretically and experimentally.[32–35] Until now no similar studies have been made regarding the stabilizing effects of halogens on *c*-BN. The halogens (especially fluorine) are generally expected to be efficient as a surface stabilizing agent due to their large ability to form strong bonds. However, the halogens must not be too strongly bonded to the surface, thereby blocking the available surface sites. They must be able to also undergo abstraction reactions with gaseous species and, hence, leave room for an incoming growth species. The mobility of the surface stabilizing agent (e.g., halogens) may also be of importance for further growth of *c*-BN. The purpose of the present work is to investigate theoretically (both structurally and energetically) the efficiency of hydrogen (H) and specific halogens (F, Cl, Br), respectively, as surface stabilizing agents during *c*-BN growth. The present work is one of the first in a series of theoretical investigations in which the underlying principles of *c*-BN vs *h*-BN nucleation and growth will be studied.

II. METHOD

A. General

Clusters of different shapes and sizes are often formed (or may be intentionally used) in the gas phase during CVD of

0163-1829/99/60(23)/16065(8)/$15.00

thin films. They are also to some extent expected to occur on the growing thin film surface. Either because of an adsorption of the gaseous cluster, or as local surface formations obtained at different stages during film growth. These clusterlike particles will then include various numbers of atoms with, hence, a large range of abilities to geometrically relax. The very small clusters will relax totally, whilst the much larger ones are expected to act more like a crystalline surface. A cluster approach and the quantum-mechanical density functional theory (DFT) method, using the program system DMOL,[36] have been used in the present investigation. The exchange-correlation functional B-LYP (Refs. 37 and 38) (Becke and Lee, Yang, and Parr) was then applied in the DFT calculations.

The following formula was used in calculating the adsorption energies:

$$E_{\mathrm{ads},X}=E_X+E_T-E_{T-X}, \tag{1}$$

where E_X, E_T, and E_{T-X} are the total energies for the different adsorbates, and for the templates T with and without an adsorbed species X, respectively. This corresponds to the adsorption process

$$T^{\bullet}+X^{\bullet}\rightarrow T-X, \tag{2}$$

where $T^{\bullet}$ is the template modeling the different c-BN (111) cluster surfaces, and $X^{\bullet}$ is the absorbed species (H, F, Cl, or Br).

B. Basis set

DMOL uses exact numerical local-density functional spherical atomic orbitals within the basis sets. The basis set used in this work is the double numeric basis set with polarization functions (dnp). The dnp basis set is equivalent to the very common analytical 6-31g^{**} basis set (a split-valence basis set with polarization functions p added to H and He, and d added to heavier atoms).[39] It is most suitable for polar compounds like BN, and, hence, it gives more accurate results.[39]

C. Template size and optimization

When modeling c-BN cluster surfaces the atoms terminating the template must then as perfectly as possible simulate an artificial continuing of the real cluster. This must also be the situation for c-BN crystal surfaces modeled as two-dimensional slabs. Hence, the first part of the investigation was to look for species that will obey this requirement, e.g., yielding the correct geometry of c-BN. For practical reasons, only small clusters were then used (see below). Hence, the atomic percentage of terminating species was also high. However, the results obtained with this type of cluster can be regarded as a lower limit. Terminating species that will yield more bulklike geometries, using this small cluster size, are also expected to lead to bulklike structural geometries for more real crystal-like surfaces. Moreover, all atoms in the clusters were allowed to be fully relaxed. A second requirement for the terminating species is that they must be sufficiently strongly bonded to the cluster surface to adequately function as terminators at elevated temperatures. On the other hand, they are not allowed to be too strongly bonded to the surface. They must be able to leave room for an incoming growth species in order for the cubic phase to continue with its growth. Thus, the second part of the present study consists of an investigation regarding surface processes such as adsorption, abstraction, and migration.

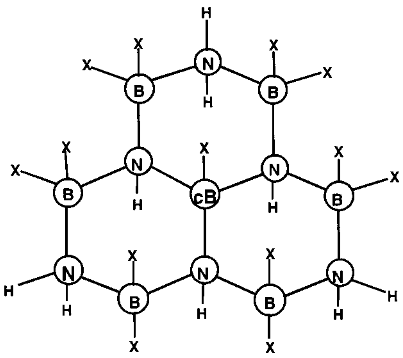

FIG. 1. A template modeling an X-terminated B(111) c-BN cluster surface (X=H, F, Cl, or Br). The same geometry is valid for N(111) cluster surfaces. However, B is then replaced by N and vice versa.

The templates used for describing two of the four c-BN clusters in the present work is $B_7N_6X_{21}$ for the B(111) cluster surface and $B_6N_7X_{21}$ for the N(111) cluster surface (Fig. 1). These clusters are equivalent to $C_{13}H_{21}$ for the isoelectronic compound diamond, which was found, using *ab initio* MO theory, to be optimal in describing a diamond (111) surface.[33,40] In the present study, X is either H, F, Cl, Br, or a combination of H and one of the halogens ($B_7N_6H_9X_{13}$ and $B_6N_7H_9X_{13}$, respectively). The latter type of termination was used for practical reasons when calculating the adsorption energies. The geometrical region surrounding the adsorption site was then terminated with halogens X, while the outer B (or N) atoms were H terminated.

Two larger templates were also used in the present study. These templates were designed to investigate the influence on structural geometry of two neighboring radical surface sites. The templates were not allowed to be fully relaxed in order to resemble a more rigid c-BN cluster. The different atoms allowed to be geometrically optimized are marked with an asterisk in Fig. 2. The templates were $B_{10}N_9H_{13}F_{15\text{-}17}$ for a B(111) surface, and $B_9N_{10}H_{13}F_{15\text{-}17}$ for a N(111) surface. The number of fluorine atoms indicates a surface with two, one, or zero radical site(s), respectively. The latter type of surface is thus completely terminated.

The reconstruction mechanism of nonterminated, homopolar covalent semiconductor (111) surfaces generally results in delocalized π-like bonding between dangling orbitals on surface atoms affecting the four topmost layers of a crystal.[41] For heteropolar, partly covalent and partly ionic, semiconductors like c-BN, the reconstruction is rather believed to occur via a charge transfer from the surface cations to the anions. The unoccupied cation states are raised in energy and the boron cations move into the bulk becoming quasiplanar sp^2 bonded. The fully occupied anion states are accordingly lowered in energy, moving the nitrogen anions outward and are thus quasipyramidal s^2p^3 bonded, giving a buckled surface.[42] A similar buckling effect in stabilizing the boron nitride nanotubes was found in a work by Blase *et al.*[43] Charge transfer from B to N in tubes of hexagonal

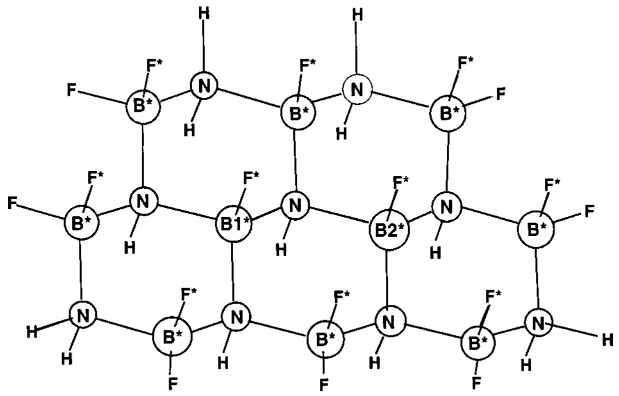

FIG. 2. A model of the larger cluster $B_{10}N_9H_{13}F_{17}$. Although here fully adsorbed, the two neighboring surface radical sites are marked with B1 and B2. Atoms marked with asterisks represent the B(111) surface layer and its adsorbed species. These atoms were allowed to relax, keeping the other atoms fixed. This simulates a more real-surface situation and the crystal character of the template is maintained as truly as possible.

BN (diameters ranging from 4 to 12 Å) lead to minimum energy structures where all the boron atoms are arranged in one cylinder and all the nitrogen atoms in a larger concentric one. More complicated types of reconstruction can also occur, such as ''vacancy buckling'' or chemisorption of trimers. Compared to the smaller clusters used in the present investigation, the larger clusters are somewhat more crystal surfacelike. The use of them is more a test of how neighboring radicals influence geometry and hybridization of one another, than a true reconstruction study, although tendencies for reconstruction may appear.

III. RESULTS AND DISCUSSION

A. General

Single bonds that form between the radical species and the surface in the adsorption process result from σ overlap between the surface dangling orbital and a corresponding orbital of the adsorbate (H, F, Cl, or Br). Fluorine has the highest electronegativity (3.98) amongst the halogens, with chlorine (3.16) and bromine (2.96) (Ref. 44) being less reactive towards other elements. Comparing the covalent radius, the situation is reversed with Br>Cl>F.[44] Fluorine therefore forms the strongest bonds with other atoms, and bromine the weakest. Hydrogen has both the smallest radius and the lowest electronegativity (2.2), giving it an intermediate position.[44]

The differences in size and electronegativity of the different terminating species will not only yield diverse bond energies for the different adsorbates investigated, but most probably also structural differences. One of the desirable roles of these adsorbates is to maintain the sp^3 hybridization of the surface atoms during growth of *c*-BN, thereby hindering the surface to collapse from a cubic to a hexagonal phase. Another role is to leave room for an incoming B- or N-containing gaseous species (growth species) for a continuous *c*-BN growth to occur. The F species is expected to be efficient as a cubic BN surface-stabilizing agent due to its large ability to form strong bonds. The Br species, on the other hand, is expected to be non-efficient due to low electronegativity and large atomic radius.

One of the main questions is, however, if surface termination is necessary in order to be able to sustain the sp^3 hybridization of the surface atoms during *c*-BN growth. Is it possible that the surface nitrogen atoms, with their lone pair electrons, should have sp^3 hybridization similar to NH_3, thereby inducing a cubic structure? As a test, a small *c*-BN cluster was not surface terminated, but allowed to be fully relaxed at the same level of theory compared to the other calculations in the present study. A totally collapsed geometrical structure was then obtained. The sp^3 hybridization of the original structure was completely converted to sp^2 hybridization. Hence, it is obvious that surface termination by a suitable species is of highest importance for a continued growth of *c*-BN.

B. Stability of B(111) *c*-BN cluster surfaces

1. Structural geometries

The geometry of the boron-rich B(111) surface of a small *c*-BN cluster is shown in Fig. 1. This geometry is also valid for the corresponding nitrogen-rich N(111) cluster surface. Angles are presented in Table I, and interatomic distances from the central atom to its nearest neighbors are presented below.

It was found that all terminating species investigated in the present study would sufficiently sustain the sp^3 hybridization of the boron-rich B(111) cluster surface. The angles $\nu_{\text{N-}c\text{B-N}}$ are all ranging between 108.8° and 111.3 (Table I). Regarding interatomic distances, only the Br-terminated cluster will result in a significantly increased distance of 1.70 Å. This is to be compared with the bulk value of 1.57 Å.[2] The other terminating species (H,F,Cl) lead to interatomic distances between 1.60 and 1.62 Å. Hence, the large species Br will most probably induce sterical hindrances on the B(111) surface due to large repulsion between the valence electrons in neighboring Br adsorbates. The repulsion is then expected to induce a lengthening of the distance between the surface and the adsorbate and, hence, a weakening of the corresponding bond strength (a less pronounced overlap between dangling bonds). In comparison to the corresponding bond length in BBr_3 an increase in the B-Br bond length of 0.12 Å was observed in the present work (from 1.87 to 1.99 Å).[45]

TABLE I. Angles (°) $\nu_{\text{B-}c\text{N-B}}$ and $\nu_{\text{N-}c\text{B-N}}$. Values in parentheses are for templates with a central radical atom.

	H	F	Cl	Br
B(111)	109.2 (118.6)	108.8 (118.6)	110.1 (118.2)	111.3 (119.4)
N(111)	113.0 (112.9)	110.8 (113.0)	109.6 (113.1)	109.9 (115.4)

TABLE II. Adsorption energies (kJ/mol) for different species on B(111) and N(111) cluster surfaces.

	H	F	Cl	Br
B(111)	106	273	244	109
N(111)	130	223	122	370

An abstraction of a central adsorbed species X, thus producing a radical surface site, resulted in a B(111) radical surface that almost totally collapsed at the radical site. The neighboring terminating atoms are thus not able to sustain the sp^3 hybridization of the radical surface atom. The angles $\nu_{\text{N-}c\text{B-N}}$ increased from (109°–111°) to about (118°–119°) (Table I). This difference gives evidence of a transition from sp^3 hybridization (109.4°) to sp^2 hybridization (120°). The radical surface site has then been stabilized by a hyperconjugation interaction.[46] This is a resonance interaction in which the radical electron in a p-type orbital on the central radical B (cB) atom interacts with an adjacent B-N bond that is aligned with it. This gives partial double bond character to the cB-N bonds and weakens the aligned B-N bonds. Several features in the present study support such resonance stabilization. First, the interatomic cB-N distance shortens from 1.70 Å in the nonradical Br terminated template to about 1.58 Å in the monoradical template. The average shortening for the different terminators, H, F, Cl, and Br is 0.10 Å. Second, the aligned B-N bonds in the Br terminated template lengthen from 1.65 to 1.72 Å (the average increase is +0.06 Å), while the other B-N bond lengths do not change.

2. Adsorption energies

The adsorption energies for the different terminating species were calculated using Eq. (1). As can be seen in Table II, the terminating fluorine and chlorine species will result in the largest adsorption energies (273 and 244 kJ/mol, respectively) for a B(111) surface. These species, being the two most electronegative elements in this investigation, experience a strengthening of the bonds by ionic-covalent resonance, either a double bond between two ions (B^+ and F^-/Cl^-) or a single bond between B and F/Cl atoms.[47] They will also satisfactorily simulate the heteropolarity of BN. The bromine atoms, being larger and less reactive, will give lower adsorption energy (109 kJ/mol) and will, as discussed above, show a tendency for induced sterical hindrances. However, the numerical value of adsorption energy is somewhat too low compared to what would be expected, especially in comparison with hydrogen and the other halogens. Hydrogen is the only terminating species that will result in an almost nonpolar bond (B and H have similar electronegativities). In comparison with the more polar (B-N) bonds of the bulk, this may weaken the B-H bond to some extent. Although H is capable to geometrically stabilize the surface geometry very well, the low adsorption energy (106 kJ/mol) makes H less suitable as a surface stabilizer.

A six-layer-thick slab with periodic-boundary conditions was also used in studying the adsorption of H and F, respectively, to a B-rich (111) surface, modeling a more realistic crystalline surface of c-BN. A supercell approach was then used. The six-layer slab was included in a unit cell with vacuum regions of 18 Å in the (001) direction, while keeping the periodicity in the (100) and (010) directions. A number of three layers of atoms were then allowed to relax, also including the surface terminating H (and F) atoms. As a result, the calculated adsorption energies for H and F, on a crystalline B-rich (111) surface, were found to be 482 and 690 kJ/mol, respectively. This is to be compared with corresponding adsorption energies for the small cluster $B_7N_6X_{21}$ (X = H or F) (106 vs 273 kJ/mol). Hence, the F species was found to bind stronger than the H species to both types of surfaces (small cluster surface vs crystalline surface). Moreover, the difference in adsorption energies between H and F was numerically the largest one for the latter type of surface. Hence, a relatively small c-BN cluster will result in an order of adsorption energies (for H and F) that is identical to the corresponding one for a more crystalline surface. The same order of adsorption energies is expected for clusterlike particles, including various numbers of atoms, on the growing c-BN surface. As already mentioned, these clusterlike particles will have a large range of abilities for geometrical relaxation, from a complete relaxation that occurs for very small clusters to a very low relaxation ability that will be the situation for a crystalline surface.

The present quantum-mechanical calculations are performed at zero Kelvin, while the real CVD process is dynamic and at a finite temperature. It is, hence, of a large interest also to investigate the stabilities of the various terminated surfaces at an elevated temperature. Molecular-dynamic calculations at 1200 K have been performed in order to study the effect of temperature on the bond strength of the different terminating species. The force constants were then obtained from quantum-mechanical calculations (DFT-based) using the program CASTEP from Molecular Simulation/Biosym Technologies of San Diego.[48] Furthermore, a step length of 0.2 fs was used in the simulations. The bond length between the adsorbate-binding surface atom and the terminating adsorbate was then regarded to be a measure of the corresponding strength. As a result, the B-H and B-F bonds were slightly increased (by about 10% and 2%, respectively). Hence, the bond strengths of the terminating H and F species on B(111) surfaces were found to be not affected much by an increase in temperature from 0 to 1200 K, especially when considering the relative bond lengths.

3. Abstraction and migration of terminating species on B(111)

The possibility of surface-terminating species to undergo abstraction reactions has also been investigated in the present study. Both the H-and F-terminated B-rich (111) surfaces were then assumed to undergo abstraction reactions, including gaseous H and F species. The template modeling a more realistic crystalline surface, one of the extremes in the present investigation, was then used for the calculations. The energetically most favorable abstraction reaction on B(111) involved surface-terminating H species. An abstraction of adsorbed H species by gaseous H was found to be a weakly endothermic process at 0 K (123 kJ/mol), which, however, will be possible to occur at elevated temperatures and at the supersaturation condition of hydrogen in chemical vapor deposition of c-BN thin films. This is to be compared with the endothermic abstraction reaction of surface-terminating F species with gaseous F (542 kJ/mol). Based on this energetic investigation, it will be possible to draw the conclusion that an X-terminated B-rich c-BN (111) surface will be energetically favorable in abstraction reactions, including the gaseous X species ($X=\mathrm{H}$).

The probability for surface migration of the various terminating species is also of large interest to study theoretically. An abstraction, or high mobility, of the terminating species is needed for a continuous growth of the c-BN phase. The migration process investigated in the present study is assumed to involve two neighboring surface radical sites on the template modeling the more realistic crystalline surface. Migration of H and F, respectively, is then assumed to occur as a single jump between the two radical surface sites. A transition state (TS) has then in the present study been located on the potential-energy surface, and the barrier of energy has then been calculated as the difference in energy between the TS and the adsorbed configuration. It was found that F is not only very strongly bonded to the crystalline B(111) surface (690 kJ/mol), but also has a very high energy for abstraction with gaseous F (540 kJ/mol). The calculated barrier of energy for the assumed migration path was calculated to also be very high (330 kJ/mol). The F atoms thus seem to block the possible growth sites on the B(111) surface. Contrary to the results obtained for F-terminated surfaces, the surface stabilizing H atoms are found to be much more mobile, either by a rather low abstraction energy (123 kJ/mol) or by a migration of H species on the surface (energy barrier of 252 kJ/mol). Both these energies are much lower compared to the corresponding situation with a F-terminated surface.

4. Radical neighbors

It is generally of much interest to study the influence of the surface radical density on structural geometry and adsorption processes. In the present work the influence of neighboring radicals on structural geometry and hybridization of the c-BN surface atoms (i.e., reconstruction) has also been investigated. A larger template that includes two neighboring adsorption sites ($B_{10}N_9H_{13}F_{15-17}$) was constructed for this purpose. It can be described as five B_3N_3 rings fused together in the chair formation (Fig. 2). Two neighboring terminating F species were then removed, leaving a diradical surface site. Consequently, a slight contraction of the three B1-N and B2-N bonds, respectively, was observed (1.48–1.51 Å). Both $\nu_{\text{N-B1-N}}$ and $\nu_{\text{N-B2-N}}$ angles were calculated to be 117.0°. This is to be compared with the somewhat larger angle $\nu_{\text{N-}c\text{B-N}}$ of 118.6° obtained for the small F-terminated radical template. The existence of a radical site (monoradical or diradical site) thus seems to result in a mixture of sp^2 and sp^3 hybridization (a partial surface reconstruction). The underlying cause of this observation was discussed in Sec. III B 1. When adsorbing a fluorine atom on one of the radical sites, the bonding surface boron (B1 or B2) will adopt sp^3 hybridization since the angle $\nu_{\text{N-B-N}}$ will decrease to 108.9°. For the still radical boron atom, the $\nu_{\text{N-B-N}}$ angle has instead increased to 118.7°, which is almost identical to the value obtained for a monoradical site on the small template (118.6°). On the fully adsorbed template both boron atoms are completely converted to a sp^3 hybridization state (108.4° and 108.5°, respectively) and all optimized B-N distances are within the range 1.61 to 1.63 Å.

In conclusion, the boron atoms are subjected to a hybridization transformation from sp^3 to sp^2 during the abstraction of F atoms, and then converted back to sp^3 upon F adsorption. Thus a restructuring of the c-BN surface from its reconstructed (collapsed) geometry has occurred.

C. Stability of N(111) *c*-BN cluster surfaces

1. Structural geometries

As described in Fig. 1, the geometry of the nitrogen-rich surface is equivalent to the boron-rich surface of the c-BN cluster. The interatomic distances are presented below, and the angles of the N(111) surface can be seen in Table I. It is shown in Fig. 1 and Table I that the sp^3 hybridization of the N(111) cluster surface was, with one exception, found to be sufficiently sustained. The angle $\nu_{\text{B-}c\text{N-B}}$ increases slightly from 109.4° up to 110.8°, 109.6°, and 109.9° when using the terminating species F, Cl, and Br, respectively. A partial transition from sp^3 to sp^2 hybridization was observed for H. The angle $\nu_{\text{B-}c\text{N-B}}$ for H increased with as much as 3.6° (up to 113.0°). This enlarged angle is consistent with the increasing double-bond character in the substrate with decreasing cN-H bond strength (increasing ‘‘surface-radical character’’). Hence, hydrogen is not so likely to sustain the sp^3 hybridization on the N(111) surface of a smaller cluster.

The interatomic distances for cN-B [from the central nitrogen (cN) to the nearest boron atom (B)] are found to be 1.59, 1.61, 1.67, and 1.71 Å for H, F, Cl, and Br termination, respectively. These distances are all larger than the value of 1.57 Å obtained for the corresponding bulk material.[2] Sterical hindrances induced by the terminating species (especially Cl and Br) are most probably responsible for these increases compared to the bulk situation.

The central terminating species X was also for this type of surface removed from the surface, producing a monoradical site. This was found to yield a local partial transition to sp^2 hybridization. The angle $\nu_{\text{B-}c\text{N-B}}$ increased, with one exception, only to about 113° for all terminating species investigated. In the case of bromine, the angle $\nu_{\text{B-}c\text{N-B}}$ increased to 115.4°. If we compare this with the B(111) radical sites, where the angle $\nu_{\text{N-}c\text{N-B}}$ were within the range 118.2–119.4° and, hence, a collapse of the cubic (111) structure occurred, we can conclude that radical sites on N(111) are only partially converted to sp^2. It is thus likely that the cubic phase of c-BN will be sustained even in the situation of a not perfectly terminated nitrogen surface.

2. Adsorption energies

The calculated adsorption energies for the N(111) c-BN clusters are demonstrated in Table II. The largest numerical value was obtained for Br(370 kJ/mol), indicating an unexpected strong bond between the surface nitrogen and the terminating bromine atom. The strong bond will most probably originate from electron cloud repulsion induced by the neighboring adsorbed Br atoms on the central adsorbed one (Fig. 1). Charge transfer was theoretically observed from the adsorbed surrounding bromine atoms to the central one, and thereby a strengthening of the cN-Br bond. The average Mulliken charges Q_{Br} of the outer Br atoms were calculated to be $+0.10$, compared to $+0.02$ for the central Br atom. For comparison, the adsorption of Br to an otherwise H-terminated N(111) was also studied. The adsorption energy obtained for Br on this surface was then 207 kJ/mol compared with 370 kJ/mol for Br on the Br-terminated N(111) surface. The adsorption energy for Br thus decreases, in contradiction with the more open adsorption site represented by the H-terminated N(111) radical surface. The Mulliken charge transfer is for this type of surface composition localized to the two central atoms alone, from the surface N atom to its Br adsorbate. There is hardly any effect on either the BN surface or the neighboring adsorbed atoms. The H atoms being smaller and ''harder'' most probably explains this. The charge transfer to the central Br atom from the neighboring H atoms is therefore negligible and owing to that, the bond-strengthening charge-transfer effect is smaller. However, guided by the geometrical results, bromine is not likely to support the stabilization of the cubic phase in a real CVD process, neither for a cluster nor for a surface. For the latter situation, there is much less freedom for surface atoms to move, and hence, bond distances to be enlarged. The second largest adsorption energy obtained in the present study for the N(111) surface is for the F termination (223 kJ/mol). Despite the reversed polarity of the adsorbate-surface bond (compared to a N-B bond), relatively strong bonds with the surface will be formed due to the large electronegativity of fluorine. The terminating H and Cl species lead to small adsorption energies (130 vs 122 kJ/mol) and will therefore most probably not play an important role in the stabilizing process of *c*-BN clusters.

A more realistic crystalline N(111) surface of *c*-BN has also been used here in studying the adsorption processes of H and F, respectively (for methodological details, see Sec. III B 2). As a result, the calculated adsorption energies for H and F, respectively, were found to be 438 vs 251 kJ/mol. This is to be compared with corresponding adsorption energies for the small cluster $B_7N_6X_{21}$ (X=H or F) (130 vs 223 kJ/mol). Interestingly, the order of adsorption energies was observed to be reversed when comparing the results obtained for a crystalline surface with those obtained for the small cluster surface used in the present study. For the crystalline surface, besides an overall increase in binding capabilities for both types of species (H and F) there is now an extreme capability for H (compared to F) to terminate the N(111) surface. Hence, the H species will be efficient as a N(111) surface-terminating agent only for larger cluster sizes with a smaller range of abilities for geometrical relaxation.

Molecular-dynamic calculations have also been performed for this type of surface, N(111), in order to study the effect of temperature on the bond strengths of the terminating H and F species, respectively. As a result, the N-H bond was slightly increased (by almost 15%). However, the N-F bond was found to be more considerably prolonged (by about 42%). Hence, it was found that an increase in temperature from to 1200 K would only affect the N-F bond appreciably, in a negative way by weakening it. The other bonds (B-H, B-F, and N-H) were found to be relatively unaffected.

3. Abstraction and migration of terminating species on N(111)

The possibility of crystalline surface-terminating species (H and F) undergoing abstraction reactions on the N(111) surface has also been investigated in the present study. The abstraction processes of adsorbed H and F species by gaseous H vs F were found to be markedly weak endothermic processes at 0 K (45 vs 28 kJ/mol. The probability of these species undergoing abstraction reactions are, hence, more pronounced for the N(111) compared to the B(111) one.

The probability of surface migration of H and F, respectively, on the crystalline N(111) surface has also been included in the present investigation (for methodological details, see Sec. III B 2.). It was found that a very large tendency for F to undergo surface abstraction reactions with gaseous F (28 kJ/mol), together with the relatively weak adsorption energy, is strongly correlated with the relatively small barrier of energy for the assumed single jump migration path (182 kJ/mol). The migration barrier of H was, however, found to be higher (312 kJ/mol), and correlating well with the high adsorption energy (438 kJ/mol). However, the abstraction energy of adsorbed H by gaseous H was unexpectedly low (45 kJ/mol), resulting in the main conclusion that H is (compared to F) very efficient as a terminating species since it has a larger probability of (i) being bonded to and, hence, stabilizing the surface, and (ii) leaving room for an incoming growth species to the N(111) surface.

4. Radical neighbors

In accordance with the B(111) cluster surface, one of the aims in the present study is to investigate the effect of neighboring radicals on structural geometry and hybridization of the *c*-BN atoms. For this purpose, a larger cluster ($B_9N_{10}H_{13}F_{15\text{-}17}$) was constructed that includes two neighboring adsorption sites. The same methodology was thereafter applied, i.e., removal of two neighboring terminating F atoms resulting in a diradical site (Fig. 2). Similarly to the B(111) surface, a contraction of the three N1-B and N2-B bonds, respectively, then occurred. These bond distances decreased from 1.57 Å to a value within the range 1.49–1.50 Å. This can be compared with the corresponding distances for the B(111) cluster, where the values ranged from 1.48 to 1.51 Å (average distance of 1.495 Å). The angles $\nu_{\text{B-N1-B}}$ and $\nu_{\text{B-N2-B}}$ were both calculated to become 113.5°. Whereas the B(111) atoms totally collapse ($\nu_{\text{N-B-N}}=118.7°$), the $\nu_{\text{B-N-B}}$ angles indicate only a partial transition to sp^2 hybridization for the N(111) atoms. This partial transition is similar to the one observed for the small cluster with one radical site, where the angle $\nu_{\text{B-}c\text{N-B}}$ was 113.0°.

One fluorine atom was thereafter adsorbed on the N1 radical site, increasing the three N1-B distances to 1.54 Å and decreasing the angle $\nu_{\text{B-N1-B}}$ to 111.5°. The angle $\nu_{\text{B-N-B}}$ on the still radical atom N2 decreased even more to 108.9°. For the fully adsorbed template, the angles $\nu_{\text{B-N1-B}}$ and $\nu_{\text{B-N2-B}}$ were 111.2° and 112.1°, respectively. The N1-B and N2-B distances were in the range of 1.54 to 1.59 Å. The reconstructed radical N(111) cluster was, hence, in the same manner as B(111) restructured again upon the adsorption of F atoms. There is one big difference, though. The sp^3 hybridization of N(111) surfaces are well sustained with a radical concentration of roughly 20% (radical sites/occupied sites). This is not the case for the B(111) cluster surfaces.

IV. CONCLUSION

The surface stabilizing efficiency of hydrogen and halogens (F, Cl, and Br) on both B(111) and N(111) *c*-BN clusters has been structurally and energetically investigated, using the quantum-mechanical DFT method. The F species was found to be very strongly bonded to both types of *c*-BN (111) cluster surfaces (273 [B(111)] vs 223 [N(111)] kJ/mol). The H species, however, showed rather small adsorption energies (106 [B(111)] vs 130 [N(111)] kJ/mol). It was observed that the very large species Br is able to induce sterical hindrance on both types of surfaces.

A more realistic crystalline surface of *c*-BN was also modeled. Significant increases in adsorption energies for the terminating H and F species, respectively, were then generally obtained. Moreover, an identical order of adsorption energies was obtained for the B(111) surface. The F species was then found to be more strongly bonded to both the smaller cluster surface, as well as to the crystalline counterpart. On the contrary, a reversed order of adsorption energy was obtained for the N(111) surface. The H species was for the crystalline surface found (in comparison with F) to be extremely effective as a surface stabilizing agent. The F species was slightly more effective on a much smaller cluster surface. Hence, the H species will be efficient as a N(111) surface-terminating agent only for larger cluster sizes with a smaller range of abilities for geometrical relaxation.

The surface-terminating species must not be too strongly bonded to the surface, thereby blocking the available growth sites. Hence, the abstraction of terminating species with gaseous ones, as well as the migration of the terminating species over the surface, have also been investigated in the present study. The calculations showed that the F species adsorbed on the B(111) surface will most probably block the surface, and thereby hinder any further *c*-BN growth. The H species was found to both efficiently stabilize the surfaces as well as having the capability to leave room for an incoming growth species to the surface.

When producing a monoradical site on the N(111) surface by abstracting the central adsorbed species on the small templates, a local partial transition to sp^2 hybridization was obtained. On the other hand, on the monoradical B(111) surfaces the transition to sp^2 hybridization for the radical site was almost complete. It is therefore possible to draw the conclusion that the cubic phase of BN will be sustained even in the situation of a not perfectly terminated N(111) surface. The B(111) surfaces need, however, to be fully occupied.

As a conclusion from all results obtained in the present investigation, the best candidate for stabilization of both B(111) and N(111) surfaces is hydrogen, H. This is especially expected to be valid during the growth of CVD thin films of *c*-BN where, e.g., the defects, microstructure, and morphology of the surfaces are governed by the incorporation and/or growth of clusterlike particles of different sizes and, hence, abilities for various degrees of geometrical relaxation.

ACKNOWLEDGMENTS

This work was supported by the Swedish Research Council for Engineering Sciences (TFR) and the Ångström Consortium. Computational results were obtained using software programs from Biosym Technologies of San Diego, first-principle DFT calculations from DMOL, DFT-based molecular-dynamic simulations from CASTEP, and graphical display using INSIGHT II.

---

[1] S. P. S. Arya and A. D'Amico, Thin Solid Films **157**, 267 (1988).

[2] L. Vel, G. Demazeau, and J. Etourneau, Mater. Sci. Eng., B **10**, 149 (1991).

[3] V. L. Solozhenko, High Press. Res. **13**, 199 (1995).

[4] D. L. Medlin, T. A. Friedmann, P. B. Mirkarimi, M. J. Mills, and K. F. McCarty, Phys. Rev. B **50**, 7884 (1994).

[5] R. H. J. Wentorf, Jr., Chem. Phys. **26**, 956 (1957).

[6] E. Yamaguchi, Mater. Sci. Forum **54-55**, 329 (1990).

[7] X. Ma, J. Yang, D. He, and G. Chen, Thin Solid Films **322**, 37 (1998).

[8] I. Konyashin, J. Bill, and F. Aldinger, Chem. Vap. Deposition **3**, 239 (1997), and references therein.

[9] F. G. Celli and J. E. Butler, Appl. Phys. Lett. **54**, 1031 (1989).

[10] I. Kim, S. Kim, and K. Kim, J. Vac. Sci. Technol. A **16**, 2295 (1998).

[11] P. B. Mirkarimi, K. F. McCarty, D. L. Medlin, W. G. Wolfer, and T. A. Friedmann, J. Mater. Res. **9**, 2925 (1994).

[12] T. Ichiki, S. Amagi, and T. Yoshida, J. Appl. Phys. **79**, 4381 (1996).

[13] T. Ichiki, T. Momose, and T. Yoshida, J. Appl. Phys. **75**, 1330 (1994).

[14] D. J. Kester and R. J. Messier, Appl. Phys. **72**, 504 (1992).

[15] K. Bewilogua, Vide: Sci., Tech. Appl. **52**, 70 (1996).

[16] D. L. Medlin, T. A. Friedmann, P. B. Mirkarimi, G. F. Cardinale, and K. F. McCarty, J. Appl. Phys. **79**, 3567 (1996).

[17] T. Yoshida, Diamond Relat. Mater. **5**, 501 (1996).

[18] D. J. Kester, K. S. Ailey, R. F. Davis, and K. L. More, J. Mater. Res. **8**, 1213 (1993).

[19] D. R. McKenzie, W. D. McFall, W. G. Sainty, C. A. Davis, and R. E. Collins, Diamond Relat. Mater. **2**, 970 (1993).

[20] D. R. McKenzie, J. Vac. Sci. Technol. B **11**, 1928 (1993).

[21] W. A. Yarbrough, J. Vac. Sci. Technol. A **9**, 1145 (1991).

[22] Y. Bar-Yam *et al.*, in *Wide Band Gap Semiconductors*, edited by T. D. Moustakas, J. I. Pankove, and Y. Hamakawa, MRS Symposia Proceedings No. 242 (Materials Research Society, Pittsburgh, PA, 1992), p. 335.

[23] A. Bartl, S. Bohr, R. Haubner, and B. Lux, Int. J. Ref. Hard Metals Hard Mater. **14**, 145 (1996).

[24] M. Kuhr, R. Freudenstein, S. Reinke, W. Kulisch, G. Dollinger, and A. Bergmaier, J. Chem. Vap. Dep. **3**, 259 (1995).

[25] Y. Guo, Z. Song, G. Li, and G. Chen, Chin. J. Phys. I **5**, 143 (1996).

[26] I. Konyashin, J. Loeffler, J. Bill, and F. Aldinger, Thin Solid Films **308–309**, 101 (1997).

[27] K. Liao and W. Wang, Phys. Status Solidi A **147**, K9 (1995).

[28] K. P. Loh, I. Sakaguchi, and M. Nishitani-Gamo, Phys. Rev. B **57**, 7266 (1998).

[29] W. Kalss, R. Haubner, and B. Lux, Diamond Relat. Mater. **7**, 369 (1998).

[30] C. Schaffnit, L. Thomas, F. Rossi, R. Hugon, and Y. Pauleau,

Surf. Coat. Technol. **98**, 1262 (1998).

[31] S. J. Harris, A. M. Weiner, G. L. Doll, and W.-J. Meng, J. Mater. Res. **12**, 412 (1997).

[32] K. Larsson, in *Diamond for Electronic Applications*, edited by D. L. Dreifus, *et al.* MRS Symposia Proceedings No. 416 (Materials Research Society, Pittsburgh, PA, 1995), p. 287.

[33] K. Larsson and S. Lunell, J. Phys. Chem. A **101**, 76 (1997).

[34] R. C. Mendes de Barros *et al.*, Diamond Relat. Mater. **6**, 490 (1997).

[35] K. Larsson and S. Lunell, Diamond Relat. Mater. **7**, 1138 (1998).

[36] DMOL program system of Biosym Technologies, Inc., San Diego.

[37] A. J. Becke, J. Chem. Phys. **88**, 785 (1988).

[38] C. Lee, W. Yang, and R. Parr, Phys. Rev. B **37**, 785 (1988).

[39] DMOL User Guide, version 2.3.0 (Biosym Technologies, San Diego, 1993).

[40] K. Larsson, S. Lunell, and J.-O. Carlsson, Phys. Rev. B **48**, 2666 (1993).

[41] P. Pandey, Phys. Rev. B **25**, 4338 (1982).

[42] G. P. Srivastava, Rep. Prog. Phys. **60**, 561 (1997).

[43] X. Blase, A. Rubio, S. G. Louie, and M. L. Cohen, Europhys. Lett. **28**, 335 (1994).

[44] D. F. Shriver, P. W. Atkins, and C. H. Langford, *Inorganic Chemistry* (Oxford University Press, Oxford, 1994), pp. 377 and 543.

[45] M. C. Ball and A. H. Norbury, *Physical Data for Inorganic Chemists* (Longman, London, 1974), p. 148.

[46] R. I. Morrison and R. N. Boyd, *Organic Chemistry* (Allyn and Bacon, Boston, 1973).

[47] F. A. Cotton and G. Wilkinson, *Advanced Inorganic Chemistry* (Wiley, New York, 1988), pp. 162 and 205.

[48] CASTEP program system of Molecular Simulation/Biosym Technologies, Inc., San Diego.